International Journal of Thermophysics, Vol. 17, No. 1, 1996

Hydrates in the Ocean and Evidence for the Location of Hydrate Formation[1]

J. P. Long[2] and E. D. Sloan[3,4]

There is substantial evidence that the oceans of the world will pose the most important challenges in the area of hydrate formation. This work indicates three areas of concern for hydrate formation in the ocean: (1) deposits of natural gas in ocean hydrates, which will serve as an energy resource and environmental concern in the next millenium, (2) a recent proposal for the ocean storage of carbon dioxide in the form of hydrates, and (3) the prevention of hydrate formation in ocean pipelines. To address such applications, fundamental knowledge on the site of hydrate formation was determined. Results are presented for quiescent, high-pressure experiments done in a sapphire tube to determine the site of hydrate formation in deionized water and in mixtures with amorphous silica and sodium dodecyl sulfate. Visual (microscope aided) results are presented for formation with a typical gas mixture and with carbon dioxide.

KEY WORDS: amorphous silica; carbon dioxide; clathrates; growth; hydrates; hypothesis; natural gas; nucleation; ocean; sodium dodecyl sulfate.

1. INTRODUCTION

Only in the last three decades has mankind recognized that the formation of *in situ* hydrates in the geosphere predated their artificial formation (1810) by several million years. In addition to their extreme age, it appears that hydrates in nature are ubiquitous, with some probability of occurrence wherever water and small (<0.9nm) molecules are in close proximity, at low temperature and elevated pressures. Because hydrates concentrate gases such as methane by a factor of 170, and because as little as 10% of

[1] Invited paper presented at the Twelfth Symposium on Thermophysical Properties, June 19–24, 1994, Boulder, Colorado, USA.

[2] Mobil Exploration and Production Technical Center, Dallas, Texas 75381-9047, USA.

[3] Center for Hydrate Research, Colorado School of Mines, Golden, Colorado 80401, USA.

[4] To whom correspondence should be addressed.

0195-928X/96/0100-0001$09.50/0

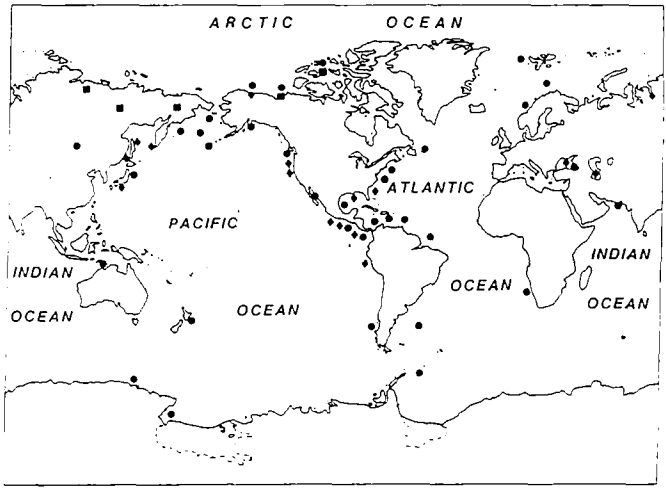

Fig. 1. Locations of *in situ* gas hydrates around the world [1].

the recovered energy is required for dissociation, hydrate reservoirs have been considered as a energy resource for the next millenium.

The most recent appraisal [1] estimates the amount of gas in hydrates at 2×10^{16} m^3, representing 53% of the organic carbon reserves in the earth. Figure 1 shows 47 locations where hydrates are expected; of these locations, 14 represent irrefutable evidence of hydrate corings. Among the total worldwide locations, 42 are in oceans, supporting the fact that ocean hydrate reserves surpass those in permafrost regions by about two orders of magnitude. Hydrates are restricted to less than 10% of the total oceanic area, generally confined to slope and rise sediments of outer continental margins below water depths of about 300 to 500 m. Three plausible means to recover gas from hydrates have been reviewed [2], with the result that depressurization (the most likely method) will not be used until after the year 2000 due to economic considerations. Kvenvolden [1] points out that these ocean hydrates can also serve as geologic hazards as well as possible causes of global warming.

A second major area of concern for hydrates in the ocean lies with the recent Japanese plan to sequester liquid carbon dioxide (CO_2) in the ocean [3], as shown schematically in Fig. 2. CO_2 is recovered from power plant stacks, liquefied, and eventually injected 3 km below the surface of the ocean, where the density of CO_2 is 13% greater than that of seawater. The thermodynamic conditions are such that CO_2 will form hydrates when it is expelled from the subsea pipe. Recently, our laboratory [4] has described alternative conditions which favor either acidification of seawater or the

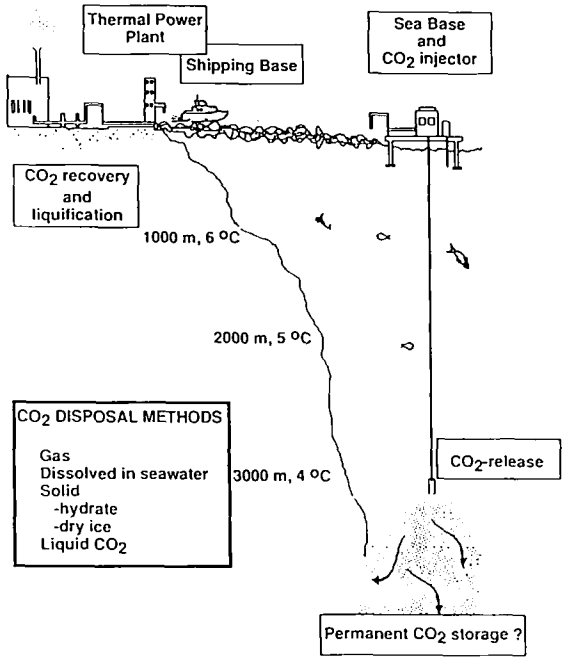

Fig. 2. Conceptual process of carbon dioxide disposal as hydrates [3].

combination of CO_2 with rocks. The CO_2 storage concept, wich was proposed in 1977 [5], has gained acceptance among the Japanese, who have published over 20 articles on the topic since 1991. The Japanese suggested that a national project on CO_2 storage might begin in 1994.

The final application of hydrates in the ocean regards the transportation of gas in an environment such as the North Sea or the Gulf of Mexico. In Northern ocean environments, and wherever such pipelines are in water deeper than 600 m, the fluids reach a temperature of about 277 K within 1 or 2 km after they evolve from the reservoir at the ocean floor. Such temperatures are suitable for hydrate formation at the pipeline pressures. Each year more than U.S. $\$500 \times 10^6$ is spent for injection of methanol in order to prevent hydrate formation in these pipelines. Further, future environmental concerns will mitigate methanol injection due to potential leakages. This effort is turning to alternative means for hydrate prevention, labeled kinetic inhibitors [6], wich are currently being field-tested and show economic promise for future inhibition schemes.

In order to address the above three challenges in ocean hydrate formation, we must apply fundamental knowledge in the form of questions, such

as (1) What are hydrates? (2) Under what conditions do hydrates form? and (3) How do hydrates form? The first two of these questions have been answered with acceptable accurancy, as presented in several reviews [7–9]. The third question, however, is only beginning to be addressed. The purpose of the remainder of this work is to present experimental results for the questions, "Where does hydrate formation normally occur under quiescent conditions?" and "How is hydrate formation affected by a high-energy surface (e.g., amorphous silica) and by a simple surfactant?"

1.1. Literature Review of Hydrate Formation Models

In the literature, only a few models exist for the mechanism of gas hydrate nucleation and growth. Four models are briefly described below.

1.1.1. The Model of this Laboratory

On the basis of hydrate nucleation from ice [10–12], Sloan and Fleyfel [13] proposed a new hypothesis to describe the molecular mechanism for gas hydrate nucleation from ice; the hypothesis was later extended to hydrate formation from water [14]. The model used a new physical parameter, namely, the guest/cavity size ratio. The model had the following five steps as shown schematically for a pressure-temperature isochoric trace in Fig. 3.

(1) Initially free liquid water exists for the formation of hydrogen bonds.

(2) Labile cavities form with the disolution of apolar molecules in water.

(3) Labile cavities link through either verticles (to form the structure I unit cells) or faces (to form the structure II unit cells).

(4) Unit crystals combined with cavities to form a large mass of hydrates.

(5) Crystals of a dimension larger than the critical size would grow without difficulty.

Once the crystals have grown beyond the critical size, the primary nucleation period ends with the initiation of monotonic growth of hydrate crystals. This was the first model to describe the hydrate formation process on a molecular scale. The concentration of each intermediate species was modeled by first-order chemical kinetics. The semiempirical model was in good agreement with available experimental data.

The model was extended by Christiansen and Sloan [15], who proposed a molecular mechanism for hydrate formation with two addi-

tions: (1) the labile clusters could transform from one coordination number to another upon joining, and (2) while cubic structure I had no other alternatives for joining hexagonal faces, cubic structure II had two other alternatives, leading to competing structures and slowing hydrate nucleation and growth process.

1.1.2. The Model of Englezos et al. [16, 17]

Based on crystallization theory and two-film theory, Englezos et al. [16, 17] developed a semiempirical model for kinetics of the methane, ethane, and methane + ethane mixture hydrate formation process. This model was recently extended [18] to electrolyte solutions. In the two-step model (1) dissolved gas diffuses from the bulk solution to the hydrate crystal + liquid interface trough a stagnant film around a hydrate particle and (2) the hydrate reaction occurs at the hydrate + water interface, incorporating gas molecules into a structured water framework. The model was found to represent the linear growth rate data well after the hydrate had nucleated to the turbidity point.

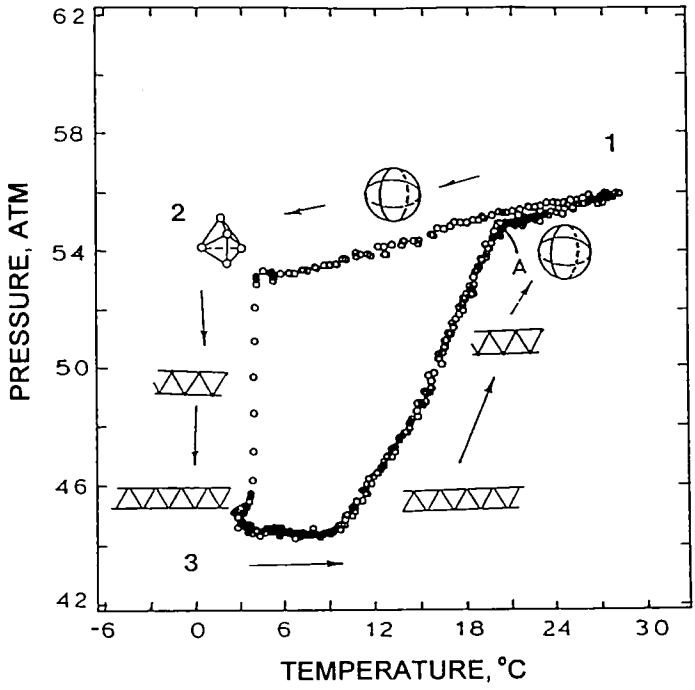

Fig. 3. Schematic of hydrate formation on an isochoric P–T trace.

1.1.3. The Model of Lekvam and Ruoff [19]

Lekvam and Ruoff [19] recently proposed that the formation and growth of methane hydrate could be described as an autocatalyctic processes. Their model was divided into five pseudoelementary reactions with the following three elements: (1) dissolution of methane gas molecules into liquid water phase, (2) buildup of a precursor of methane hydrate, and (3) growth of methane hydrate by an autocatalyctic process. The Lekvan-Ruoff model covered the whole spectrum of the hydrate formation process, from dissolution of gas molecules into the liquid water phase to crystal growth, but experimental validation was not available.

1.1.4. Experimental Observations of Burruss [20]

Burruss [20] showed that gas hydrate can form from the bulk solution of natural inclusion of carbon dioxide or methane for special conditions. In his system, the volume of the natural inclusion sphere was small (less than 100 μm in diameter) and the solution salinity was high (greater than 18% wt NaCl) at 233 to 243 K. However, the hydrate formation conditions due to the system's small size and wall effects may be significantly different than those for a larger system. To date, there is no evidence that hydrates can form in the interior bulk liquid phase at operating conditions above 273 K, with a relatively large system.

Since many of the above models suggested that hydrate formation could occur either at the surface or in the bulk, we set about to determine where hydrate formation did occur, with the construction of an apparatus and experiments described in the following section.

2. MEASUREMENTS

The objectives for this portion of the work were to locate visually where gas hydrate growth occurs and to examine the growth pattern and the morphology of gas hydrates. Only an abbreviated description is given here; the reader is refered to the thesis of Long [21] for more detail.

2.1. Apparatus and Chemicals

Figure 4 shows a schematic of the apparatus. The heart of the apparatus was a quiesent sapphire cylinder, rated at 69 MPa, with an inner diameter of 0.64 cm, a wall thickness of 0.64 cm, and an inner volume of 1.0 cm^3. The sapphire was mounted on a brass base with O-ring seals at both ends. The reactor was submerged into an isothermal bath with water as the cooling medium. Both the temperature and the pressure of the reactor were monitored continuously by a computer data aquisition system and

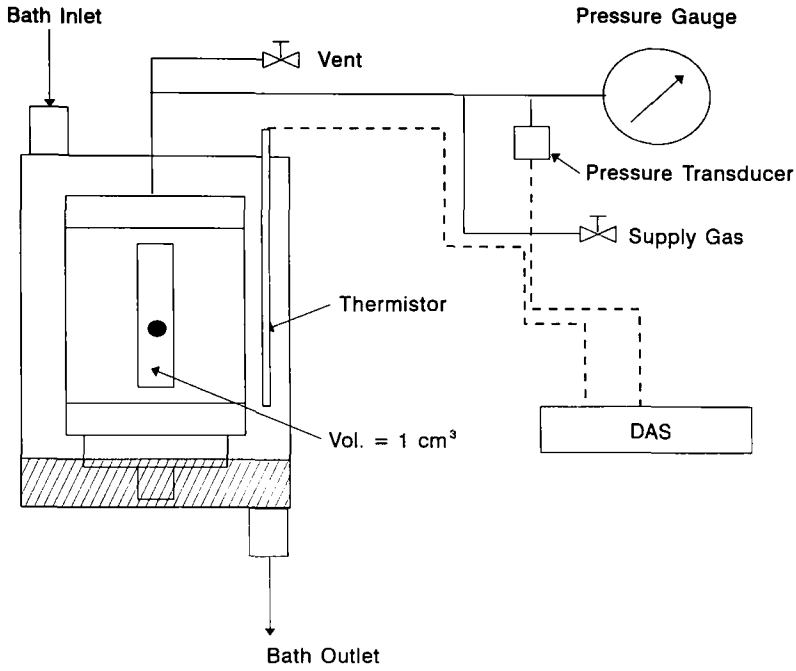

Fig. 4. Schematic of sapphire tube experimental apparatus.

encoded on videotape by a microscope-video encoder-decoder. Keithley 500 system and IBM PC-XT computers were used for data acquisition of P, T, and time. The pressure was also monitored by a Heise gauge.

The natural gas used was a synthetic Green Canyon gas (typical of the Gulf of Mexico) with the following molar composition: 87.2% methane, 7.6% ethane, 3.1% propane, 0.5% isobutane, 0.8*n*-butane, 0.4% nitrogen, and 0.4% *n*-pentane. Carbon dioxide of 99.9% purity was used where indicated. Sodium dodecyl sulfate with a purity of 98% was purchased from Aldrich Chemical Company, Inc. Deionized water and FK-500-LS synthetic amorphous precipitated slica from the North America Silica Company were also used.

2.2. Procedure

After a thorough cleaning, 0.4 cm^3 of solution was added to the reactor with a 3.0-cm^3 syringe, and the system was sealed and equilibrated for 1 h at the operating pressure with the experimental gas at ambient temperature. The cooling water valve was opened to start the experimental run by bringing the system rapidly to 277 K. Meanwhile the data acquisition

system and the video recorder were started. Observations were made via microscope during the experiment as well as with the video recorder.

3. RESULTS

Four sets of results were obtained for hydrate formation from natural gas with deionized water, amorphous silica, and sodium dodecyl sulfate (SDS), and for carbon dioxide with deionized water. The amorphous silica experiments were undertaken to study the effect of a surface on nucleation. The carbon dioxide experiments were to study the effect of a gas with two orders of magnitude higher solubility than a normal hydrocarbon, as well as to provide some background for the Japanese storage system, mentioned above. The SDS study was aimed at determining the effect of a simple surfactant blockage of surface as in catalyst poisoning.

3.1. Deionized Water with Green Canyon Natural Gas

Results were obtained for five runs with this system at 277 K and 6.9 MPa as typified in Fig. 5. In three of five experiments, hydrate nucleation initiated at the center of the gas + water interface as shown in Fig. 5. In the other two experiments, hydrate nucleation began at the edge of the gas + water interface. In all five experiments, further hydrate growth occured toward the gas side of the interface propagating across the whole surface within 10, a very small amount of gas hydrate formed in the surface region (the pressure drop was less than 7 kPa). After this rapid formation of a solid hydrate barrier on the surface, transport of gas through the hydrate film essentially stopped, as did the hydrate growth process.

After surface nucleation and growth stopped, a small amount of water came from the region beneath the hydrate film and formed hydrate along the wall of the reactor on the gas side of the hydrate interface. This process was believed to be driven by capillary forces since there were small pores

Table I. Experimental Results of Deionized Water with Green Canyon Gas at 277 K and 6.9 MPa in a Sapphire Cell (Static Conditions)

Run No.	T (K) $\pm$ 0.1	P (MPa)	Induction time (min)	Location of nucleation and growth	Amount of hydrate
1	277	6.99	4.5	Surface nucleation, surface growth	dp < 7 kPa
2	277	6.98	22.5	Surface nucleation, surface growth	dp < 7 kPa
3	277	6.98	11.8	Surface nucleation, surface growth	dp < 7 kPa
4	277	6.96	22.4	Surface nucleation, surface growth	dp < 7 kPa
5	277	6.96	N/A	Surface nucleation, surface growth	dp < 7 kPa

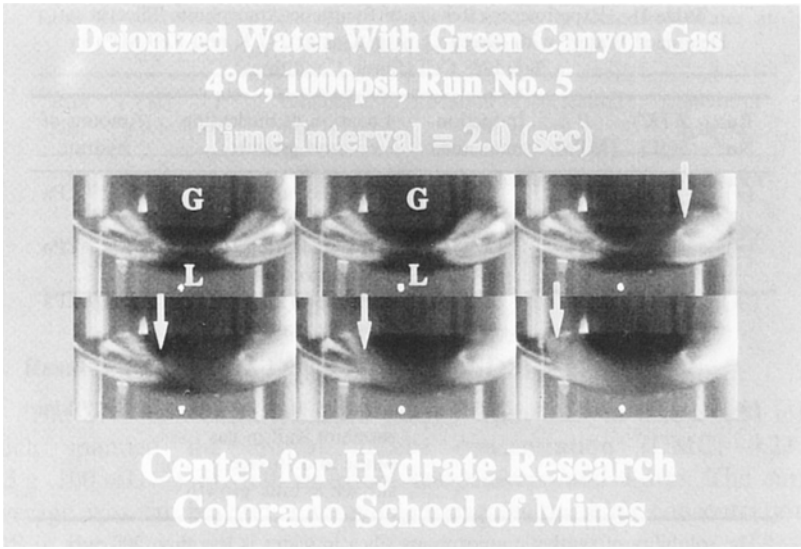

Fig. 5. Hydrate formation with deionized water at 277 K and 6.99 MPa.

between hydrates and the sapphire wall. In the bulk liquid water, small needle hydrates grew on the liquid water side of the interface (hydrate + liquid water) due to dissolved gas molecules in the liquid water. The majority of the liquid water remained clear throughout the experiments, indicating that no crystals were in the solution.

It was worth noting that only a small additional amount of hydrate formed in the experiments over a long period of time (> 24 h). The total pressure drop over 24 h was still less than 7 kPa. There was no significant hydrate growth after the first few minutes, because the impermeable solid hydrate film acted like a physical barrier between the gas and the liquid water. A summary of deionized water runs is listed in Table I.

3.2. Amorphous Silica in Deionized Water and Green Canyon Natural Gas

The purpose of this set of experiments was to study how foreign particles, such as synthetic amorphous silica particles, would influence the hydrate formation process. Two silica concentrations (200 wt ppm and 25 vol%) were used, with the latter containing most of the silica as a separate solid phase in the liquid water at the bottom of the reactor. Four experiments were conducted. In the first two experiments only a very small amount of gas hydrates formed at the gas–water interface, similar to those shown in Fig. 5. In the third experiment (with 25 vol% silica) a much

Table II. Experimental Results of Synthetic Amorphous Silica in Deionized Water[a] with Green Canyon Gas at 277 K and 6.89 MPa in a Sapphire Cell (Static Conditions)

Run No.[b]	T (K) ±0.1	P (MPa)	Induction time (min)	Location of nucleation and growth	Amount of hydrate
(*)1	277	6.96	12.3	Surface nucleation, surface growth	dp < 7 kPa
(*)2	277	6.94	137.0	Surface nucleation, surface growth	dp < 7 kPa
(+)3	277	6.96	27.5	Nucleation at sapphire wall in gas phase and surface, surface growth	dp < 7 kPa
(+)4	277	6.90	248.5	Nucleation at sapphire wall in gas phase and surface, surface & bulk growth	dp ≈ 27 kPa

[a] The solubility of synthetic amorphous silica in water is less than 200 ppm.
[b] (*) indicates a synthetic silica concentration of 200 ppm weight. (+) indicates a synthetic silica concentration of 25% by volume.

larger amount of gas hydrate nucleation and growth occured at the gas + water interface; the solid gas hydrates film prevented the gas + water contact and subsequent gas hydrate growth. There were more hydrates formed in the fourth experiment in which gas hydrate formation started from both the gas + water interface and the gas + sapphire wall in the gas phase. A summary of the four runs is listed in Table II.

3.3. Deionized Water with Carbon Dioxide

Two sets of CO_2 experiments were carried out at 288 K and 3.44 MPa, slightly below the dew point pressure (3.58 MPa). After an induction time of almost 7 h, hydrate formation started at the gas + water interface and propagated very rapidly along the wall of the reactor in the liquid water phase. The hydrate growth front moved toward the bottom of the reactor (liquid side). Downwall growth indicated that there was sufficient CO_2 present in the bulk liquid water due to its solubility. There was no hydrate growth in the gas phase. The hydrate crystal rearranged its structural appearance over more than 11 h. This was the first experiment in wich we did not observe any hydrate growth toward the gas phase. The rate of hydrate growth in the bulk water was much faster than that of natural gas hydrates due to the high solubility of CO_2. CO_2 hydrate began formation at the gas + water interface despite its high solubility in the bulk water. The summary of the runs is listed in Table III.

Table III. Experimental Results of Carbon Dioxide in Deionized Water at 273.2 K and 3.44 MPa

Run No.[b]	T (K) ± 0.1	P (MPa)	Induction time (min)	Location of nucleation and growth	Amount of hydrate
1	273.2	3.42	465	Surface nucleation, bulk growth	dp $\approx$ 7 kPa
2	273.2	3.44	$\approx$480	Surface nucleation, surface growth	dp $\approx$ 7 kPa

3.4. Results with Sodium Dodecyl Sulfate (SDS)

The SDS concentration used ranged from 0.25 to 0.20 g · 100 mL^{-1} which spanned the critical micelle concentration (CMC; 0.23 to 0.25 g · 100 mL^{-1}) of SDS at room temperature and 1 atm. The surface coverage was far beyond a monolayer due to the high concentration of SDS in the solution.

We performed a total of seven experiments using SDS with deionized water at 277 $\pm$ 0.1 K and 6.99 $\pm$ 0.03 kPa. The SDS layer blocked the gas + water interface completely, resulting in gas hydrate nucleation at three places: (1) the water + bottom metal surface with a very slow growth in the bulk water (Table IV); (2) the gas + sapphire wall surface (Table V), and (3) the water immediately below the gas + water + SDS interface with dendritic growth (Table VI). Eventually, the system with SDS formed more gas hydrate (almost all water was consumed) and the pressure drop was about 70 kPa due to convective flow of water along the sapphire wall.

4. CONCLUSIONS

We can conclude that hydrate nucleation and growth occured at (or near) the gas + water interface. Synthetic amorphous silica did not significantly impact the location of gas hydrate formation. Carbon dioxide hydrate also started formation at the gas + water interface; a gas with such a high solubility was not capable of initiating hydrate formation in bulk water. Since gas hydrates were formed easily at the gas + water interface in our quiescent system, surface renewal (e.g., through mixing or turbulence) may have a large impact on gas hydrate formation processes.

With a good surface coverage by SDS, we were able to initiate gas hydrate from the gas + water + bottom metal surface. The gas hydrate formed at the interface of water with the bottom metal and grew in the interior bulk water phase. We found that a simple surface-active agent such as SDS can significantly retard growth in a quiescent system. However,

Table IV. The Results of Gas Hydrate Formation with SDS at 6.9 MPa in a Sapphire Cell (Static Conditions)

Run No.	T (K) (± 0.1)	Location of nucleation & induction time	Hydrate growth in bulk liquid phase	Hydrate growth after convection flow
1	277.0	>15 h	No hydrate	No hydrate
	273.8	3 h after temp. reaches 0.5°C	Slow hydrate growth, dp = 7 kPa in 8h, translucent hydrate	Rapid hydrate growth, dp = 70 kPa in 1 min, massive amount of hydrate
2	277.0	3.5 h	Slow hydrate growth, dp = 7 kPa in 8 h, translucent hydrate	Rapid hydrate growth, dp = 70 kPa in 1 min, massive amount of hydrate

Table V. The Results of Gas Hydrate Formation at the Gas–Sapphire Wall with SDS at 6.9 MPa and 4.0°C in a Sapphire Cell (Static Conditions)

Run No.	P (MPa)	Location of nucleation and induction time	Hydrate growth along the wall	Hydrate growth after convection flow
1	6.98	Sapphire wall–gas, 71 min	Small amount hydrate, dp < 7 kPa, fast rate	Large amount hydrate, dp ≈ 70 kPa (1 min)
2	6.97	Sapphire wall–gas, 118 min	Small amount hydrate, dp < 7 kPa, fast rate	Large amount hydrate, dp ≈ 70 kPa (1 min)
3	6.99	Sapphire wall–gas, 117 min	Small amount hydrate, dp < 7 kPa, fast rate	Large amount hydrate, dp ≈ 70 kPa (1 min)

Table VI. The Results of Gas Hydrate Formation Below the Gas–Water–SDS Interface at 6.9 MPa and 4.0°C in a Sapphire Cell (Static Conditions)

Run No.	P (MPa)	Location of nucleation and induction time	Dendritic hydrate growth into water phase	Hydrate growth after convection flow
1	7.00	Near gas–water–SDS interface, 10.5 min	Small amount hydrate, dp < 7 kPa (≈ 4.5 min)	Large amount hydrate, dp ≈ 70 kPa (< 1 min)
2	7.00	Near gas–water–SDS interface, 9.0 min	Small amount hydrate, dp < 7 kPa (≈ 3.5 min)	Large amount hydrate, dp ≈ 70 kPa (< 1 min)

SDS did not work as an inhibitor, due to convective flow of water along the sapphire wall. A small amount of SDS increased the hydrate formation rate (mass transfer rate) significantly by convective flow.

ACKNOWLEDGMENTS

The support from the following organizations for the Center for Hydrate Research is gratefully acknowledged: Amoco, ARCO, Chevron, Conoco, Department of Energy, Exxon, Marathon, Mobil, National Science Foundation, Oryx, Petrobras, Phillips, Shell, Statoil, and Texaco.

REFERENCES

1. K. A. Kvenvolden, in *International Conference on Natural Gas Hydrates*, E. D. Sloan, J. Happel, and M. Hnatow, eds. (N.Y. Acad. Sci., New York, 1994), p. 232.
2. G. D. Holder, V. A. Kamath, and S. P. Godbole, *Annu. Rev. Energy* **9**:427 (1984).
3. I. Aya, K. Yamane and N. Yamada, in *Proceedings of the First* (1991) *International Offshore and Polar Engineering Conference*, J. S. Chung, B. J. Natvig, K. Kaneko, and A. J. Ferrante, eds. (Edinburgh, 1991), p. 427.
4. W. Harrison, R. Wendlandt, and E. D. Sloan, *App. Geochem.* (accepted).
5. C., Marchetti, *Climat. Change* **1**:58 (1977).
6. J. P. Lederhos, J. P. Long, A. Sum, R. L. Christiansen, and E. D. Sloan, in *Proceedings 73rd Annual Convention Gas Processors Association*, New Orleans (1994), p. 85.
7. D. W. Davidson, in *Water: A comprehensive Treatise, Vol. 2*, F. Franks ed. (Plenum Press, New York, 1973), p. 115.
8. E. D. Sloan, *Clathrate Hydrates of Natural Gases*, (Marcel Dekker, New York, 1990).
9. P. Englezos, *I & EC Res.* **32**:1251 (1993).
10. R. M. Barrer and D. J. Ruzicka, *Trans. Faraday Soc.* **58**:2262 (1962).
11. B. J. Falabella, *A Study of Natural Gas Hydrates*, Dissertation (University of Massachusetts, 1975) (University Microfilms, No. 76-5849, Ann Arbor, MI).
12. E. D. Sloan, *Proceedings, 69th Annual Convention Gas Processors Association*, Phoenix, AZ (1990), p. 8.
13. E. D. Sloan and F. Fleyfel, *AIChE J.* **37**:1281 (1991).
14. B. Müller-Bongartz, T. R. Wildeman, and E. D. Sloan, *Proc. 1992 2nd Int. Offshore Polar Eng. Conf.*, J. S. Chung, B. J Natvig, K. Kaneko, and A. J. Ferrante, eds. (San Franscisco, 1992), p. 628.
15. R. L. Christiansen and E. D. Sloan, in *International Conference on Natural Gas Hydrates*, E. D. Sloan, J. Happel, and M. Hnatnow, eds. (N.Y. Acad. Sci. New York, 1994), p. 283.
16. P. Englezos, N. Kalogerakis, P. D. Dholabhai, and P. R. Bishnoi, *Chem. Eng. Sci.* **42**:2647 (1987).
17. P. Englezos, N. Kalogerakis, P. D. Dholabhai, and P.R. Bishnoi, *Chem. Eng. Sci.* **42**:2659 (1987).
18. P. D. Dholabhai, N. Kalogerakis, and P. R. Bishnoi, *Can J. Chem. Eng.* **71**:74 (1993).
19. K. Lekvam and P. Ruoff, in *International Conference on Natural Gas Hydrates*, E. D. Sloan, J. Happel, and M. Hnatow, eds. (N.Y. Acad. New York, 1994), p. 558.
20. R. C. Burruss, USGS personal communication, June 1 (1993).
21. J. P. Long, *Gas Hydrate Formation Mechanism and Kinetic Inhibition*, Dissertation (Colorado School of Mines, Golden, 1994).